Kufa Journal of Engineering
Vol. 9, No. 2, April 2018, PP. 45-56
Received 17 May 2017, accepted 3 July 2017

DESTABILIZATION HEAT TREATMENT EFFECT ON EROSIVE WEAR CHARACTERISTICS OF HIGH CHROMIUM WHITE CAST IRON

Israa F. Yousif[1] and Ali H. Ataiwi[2]

[1] MSc. Student, Faculty of Engineering, University of kufa, Al-Najaf, Iraq. Email: israaf.alshannoon@student.uokufa.edu.iq

[2] Prof., University of Technology, Baghdad, Iraq. Email:130001@uoktechnology.edu.iq

http://dx.doi.org/10.30572/2018/kje/090204

ABSTRACT

In the present investigation, erosive wear property of high chromium white cast irons (HCWI) is reported. HCWI were destabilized at two different temperatures of 955^{o}C and 1100°C, air cooling followed by tempering heat treatment at 400°C and 700°C at each destabilized temperature. Erosion damage was evaluated by the removed material mass at impact angle 45° and time of 10 Hours. The surface metal flow was observed. Surface morphology of each specimen was characterized with scanning electron microscopy (SEM). The effect of heat treatment on differences in wear features of specimens is discussed. Experiment showed that the erosion rate of specimen destabilized at 1100°C, air cooled followed by tempering at 400°C air cooling is the best than other treatments. The hardness of test surface by this treatment increased from the initial 57 to 58 HRC after 10 hour. It showed that austenite in the surface structure has been transformed to martensite , which hardened the surface. Similarly, work-hardening effect also occurred on specimen destabilized at 955°C, air cooled followed by tempering at 400^{o}C, air cooling to make its surface hardness increased to 59 HRC. It was shown that HCWI series heat treated at 955°C and 1100°C and tempered at 400°C have a very good erosive wear resistance and they are expected to find wide application as wear-resistant materials.

KEYWORDS: high chromium white cast iron; Heat treatment; Microstructure; Hardness; Wear resistance; Work hardening

1. INTRODUCTION

Slurry erosion is caused by the interaction of solid particles suspended in a liquid and a surface which experiences loss of mass by the repeated impacts of particles. It is one of the main sources of failure of several slurry equipment and hydraulic components used in many industrial applications (Al-Bukhaiti et al., 2007; Llewellyn et al., 2004). Therefore, there is an urgent need to solve this problem or at least minimize its effects. The slurry erosion is a complex phenomenon and it is not yet fully understood because it is influenced by many factors, which act simultaneously. These factors include flow field parameters, target material properties and erodent particle characteristics. Among these parameters, the impingement angle and microstructure of the target material play an important role on the material removal process (Al-Bukhaiti et al., 2007). According to the literature, the microstructure of the high-chromium white cast irons, influences the wear behavior. In order to obtain a better wear performance, the high chromium white cast irons should present a martensitic structure, because the martensitic formation, compared to the austenitic, minimizes cracking and removal during wear. While it was considered that the presence of residual austenite in the microstructure causes volumetric expansion which may also lead to microcracks because of the developed stresses, some investigations determined that a certain percentage of retained austenite could improve the abrasion resistance, due to its work-hardening properties, ductility and thermodynamic metastability at room temperature (Doğan et al., 1997; Liu et al., 2008). Therefore, the microstructure must present a tough matrix and high volume fraction of hard chromium carbides, such as a high carbon hard martensite matrix hardened by secondary carbides, because retained austenite reduces the hardness which might lead to a decrease in the abrasion resistance" (Çetinkaya, 2006; Tang, 2011; Higuera-Cobos et al., 2016).

Superior erosion and abrasion wear resistance, combined with relatively low production costs, make high-chromium white cast irons particularly attractive for applications where extreme erosion and abrasion resistance is necessary. These exceptional properties are a result of the solidified microstructure, consisting of a high volume fraction of a eutectic hard carbides typeM_7C_3 (where M represents the metallic species, Fe and Cr mainly) in a softer iron matrix.

It is these carbides that are believed to give the cast iron its excellent wear resistance, whilst the ductile matrix gives the alloy a reasonable impact resistance (Adler and Doğan, 1999; Sapate and Rao, 2004). Unfortunately, there are only few slurry erosion studies on material with complex structures such as high-Cr white cast irons, in spite of them being popular wear-resistant materials.

In this research, heat treatment modifications were conducted to improve the wear properties of high chromium white cast irons that were used for mining applications and contained C 2.5% and Cr 27%. The microstructural evolution and the changes in hardness, and wear resistance, of these materials were investigated.

2. EXPERIMENTAL DETAILS

2.1. Testing machine

A jet erosion machine has been constructed according to ASTM Standard (ASTM, G73-10, 2010; G76-13, 2013) and was used to test the erosion of specimens in this research. Slurry jet erosion tester apparatus is showed in Fig. 1.

2.2. Materials and Heat treatment

The samples were cut from the casting made from high chromium cast iron, with the chemical composition shown in Table1.

Four specimens with dimensions 25mm x 20mm x 10mm were cut from the casting. They were subjected to hardening treatment in different temperatures, and then tempered. The parameters of heat treatment are shown in Table 2.

Table 1. The chemical composition of chromium cast iron (wt.%).

White Iron	C%	Si%	Mn%	P%	S%	Cr%	Mo%	Ni%	Co%	Cu%	Fe%
27Cr	2.5	0.867	0.678	0.035	0.04	27.5	0.1	0.194	0.18	0.159	Bal.

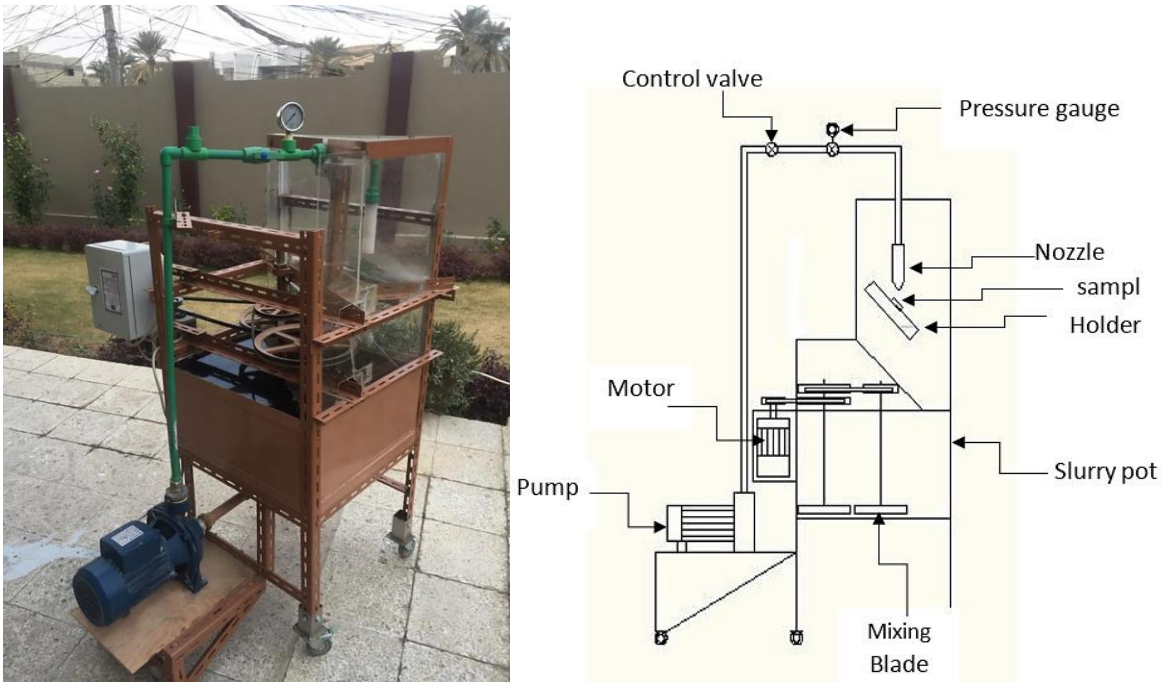

Fig. 1. slurry jet erosion tester apparatus.

Table 2. Heat treatment parameters for individual specimens.

No.	Sample name	annealing	destabilizing	Tempering
1	194A	950°C 1h/ slow cooling In furnace	955°C/ 3h/ air cooling	400°C/ 1h/air cooling
2	114A		1100°C/ 3h/ air cooling	
3	197A		955°C/ 3h/ air cooling	700°C/ 1h/air cooling
4	117A		1100°C/ 3h/ air cooling	

2.3. Metallography

Materials used in this research were characterized by optical microscope (OM). The specimens measuring 25mm×20mm×10mm were used for metallographic processing. The grinding was finished with silicon carbide paper to p3000. The polishing was carried out on the diamond-polishing machine to obtain a surface finish of 1µ. Next the polished specimens of objective materials were etched by 1.5 g copper (II) chloride in a solution of 33 ml concentrated HCl, 33 ml absolute ethanol and 33 ml distilled water.

Finally, optical microscope was used to evaluate the various phases in the microstructure of selected specimens. The metallographic structures of the alloys are shown in Fig. 2.

2.4. Hardness measurements

The specimens prepared for OM and SEM were also used for the hardness measurements. At each stage of the heat treatment hardness of each was measured by Rockwell hardness tester. Rockwell hardness testing was performed on unetched specimens using 150 kgf load (HRC150). The mean values are based on 3 different areas.

2.5. Erosion test

A jet erosion machine was used to test the erosive wear of target materials in the present investigation. silica sand (5 kg) with average diameter (600-800µm), were used as impact particles. The impact particles were changed after each test because the particles themselves also were eroded, changing the size of the particles. The specimens measuring 375mm×20mm×10mm were used for erosion test. The specimens were mounted into the test stage directly below the nozzle with a vertical distance of 10mm from the end of the nozzle to the test surface into the erosion test machine at impingement angles 45^{o}. The examined pressure was 2.5 bar. All the erosion tests were conducted at room temperature in 10 hours. Before and after the test the amounts of specimens were weighed with an electronic scale with an accuracy of ± 0.0001 g to prepare for measurements of mass loss.

3. RESULTS AND DISCUSSION

3.1. Microstructure

After destabilization treatment, the matrix structure changed from austenite to martensite and precipitation of secondary carbides can be seen clearly. Generally, when the specimen was heated to and held at the destabilizing temperature, the austenitic matrix would transform to martensite during the cooling process. However, the content and distribution of martensite matrix and secondary carbide precipitation were dependent on the quenching temperature and soaking time. The microstructures obtained after the heat treatments applied to the alloy were given in Fig. 2. By heat treatments the microstructures consisted of secondary carbide precipitates in the tempered martensitic matrix and small amount of residual austenite.

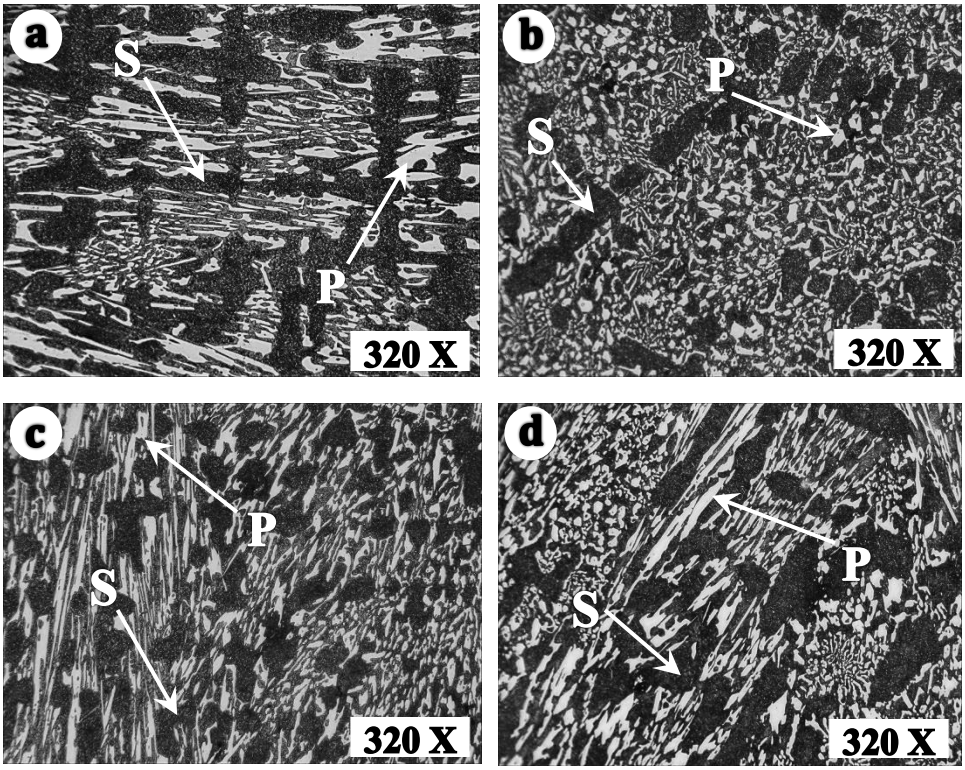

Fig. 2. Metallographic structures of the alloys (a) 194A (b) 114A (c) 197A (d) 117A, where the letter S denotes (secondary carbides precipitated in tempered martensitic matrix) and the letter P denotes (Primary carbides).

3.2. Erosion rate

Fig. 3 shows the mass loss of specimens as a function of erosion time for irregularly shaped silica sand particles at incidence angle of 45^{o}. the mass loss is approximately linear with erosion time. It can also be observed that 114A show far flatter lines than 197A and 117A. It indicates that 114 have higher erosive wear resistance and have longer life span than 197A and 117A.

To make clear the erosive wear behaviors of selected specimens, the eroded surfaces were pictured by the digital camera after the erosion tests were finished. The features were shown in Fig. 4. It is observed that eroded area of the three specimens are larger athan size of eroded surface areas of 114A.

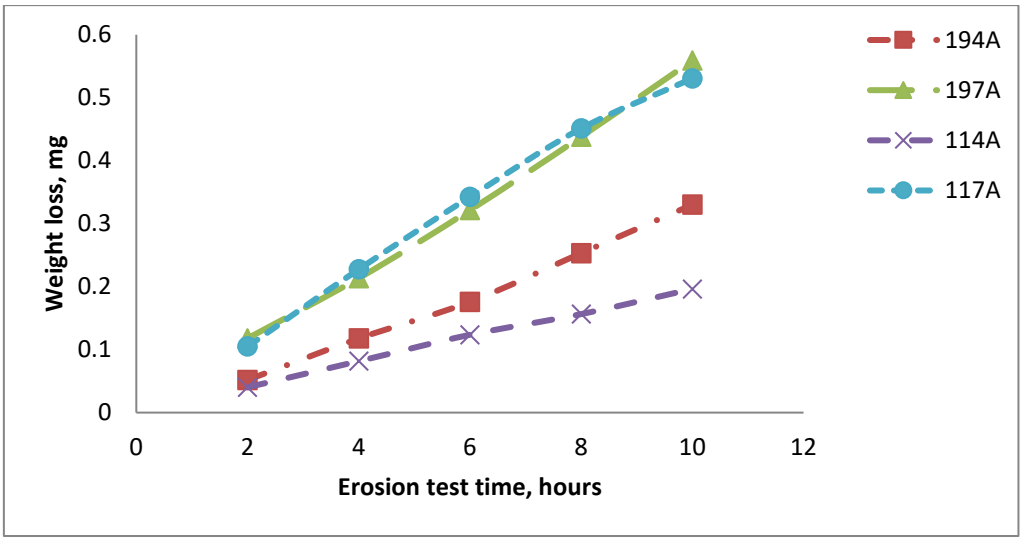

Fig. 3. Erosion test time vs. mass loss in specimens at 45°

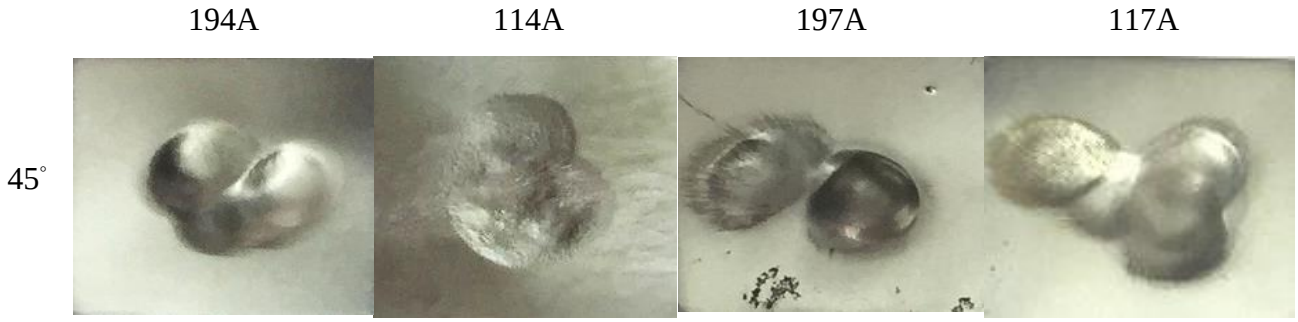

Fig. 4. Eroded surface of specimens by silica sand particles.

3.3. SEM of specimens

SEM morphologies at impact angle of 45° for specimens are shown in Fig. 5 (b) the surface featured evident cutting produced by angular particles and some ploughing. Fig. 5 (a) material displaced by ploughing is more evident along with a number of craters and shear lips. For specimens (c and d) on the other, there was a combination of damage causing deeper grooves and more material pile-up.

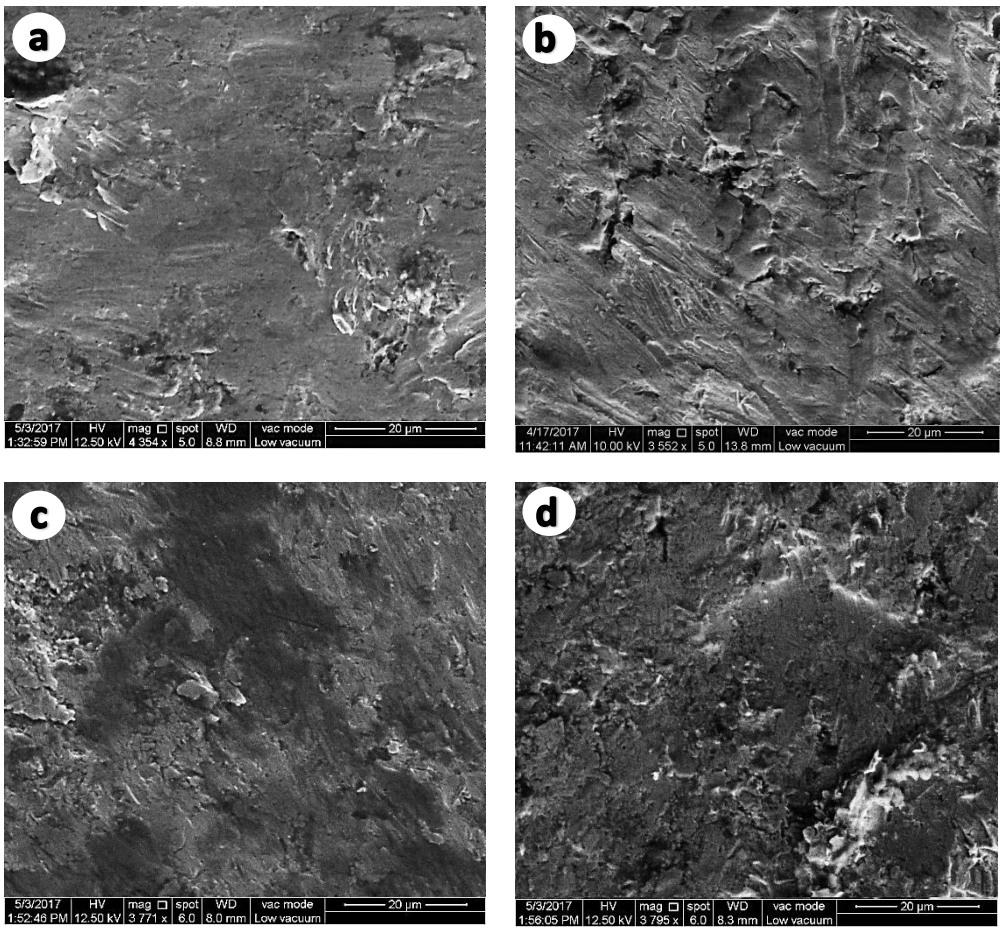

Fig. 5. SEM of eroded surface of specimens at 45º by silica sand particles (a) 194A (b) 114A (c) 197A (d) 117A

3.4. Rockwell hardness of specimens

In the erosion test, it is recognized that the work-hardening effect which resulted from impact of solid particles on material surface was happened. The hardness of specimens before and after erosion test were measured through Rockwell hardness test.

Fig. 6 shows the results of them. From the differences of hardness before and after test, we can see that there were happened the work-hardening effects on the material surface. In 194A and 114A which both have better wear-resistant properties, the results of Rockwell hardness were slightly increased after erosion test the increment of hardness may be due to strain hardening. The surface hardness of 194A increased from the initial 57 HRC to 59 HRC after 10 h of blasting. Moreover, that of eroded 114 reached to 58 HRC from the initial hardness of 57 HRC.

While although the initial hardness of 197A and 117A it almost not increased after erosion test and were more eroded than two other specimens. From this fact, we can understand that it is true that erosion rate depends heavily on hardness of surface of material (Yaer et al., 2008),

however, compare with the initial hardness of material, the hardness after work hardened is likely to be of more importance.

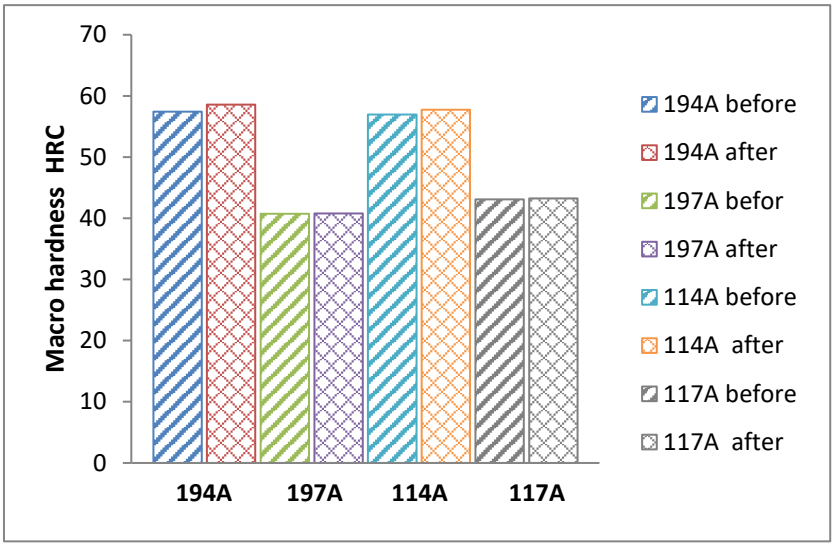

Fig. 6. Rockwell hardness for specimens before and after erosion test.

3.5. X-ray diffraction analysis

Fig. 7 (a and b) illustrate the XRD patterns for both annealed and destabilized conditions at 1100oC air cooled followed by tempering at 400oC (specimen 114A), which indicated that the samples mainly consisted of ferrous ferrite matrix and Cr7C3 carbides. It was confirmed that austenite phase expected in the structure had transformed into martensite after the heat treatment. A small amount of retained austenite was observed, consistent with the reported results (Higuera-Cobos et al., 2016; Zhi et al., 2008; Gasan and Erturk, 2013). Fig. 7 (a) shows the annealed condition before destabilization and tempering heat treatment, the alloy contained Cr7C3 and ferrite. After destabilized condition at 1100°C air cooled followed by tempering at 400°C for specimen 114A martensitic phase has appeared in addition to retained austenite as shown in Fig. 7 (b). From the results the increase of wear resistance was to increase in hardness which is further attributed to the transformation of austenitic matrix into martensite and by the precipitation of secondary carbides during tempering. By referring to Fig. 7 a and b the structure of 114A consist of M7C3, and martensite, while structure of annealed specimen consist of M7C3 and ferrite. It is known that the hardness of ferrite is lower than that of martensite. The presence or dipresence of these phases explain the reason of high wear resistance of 114A.

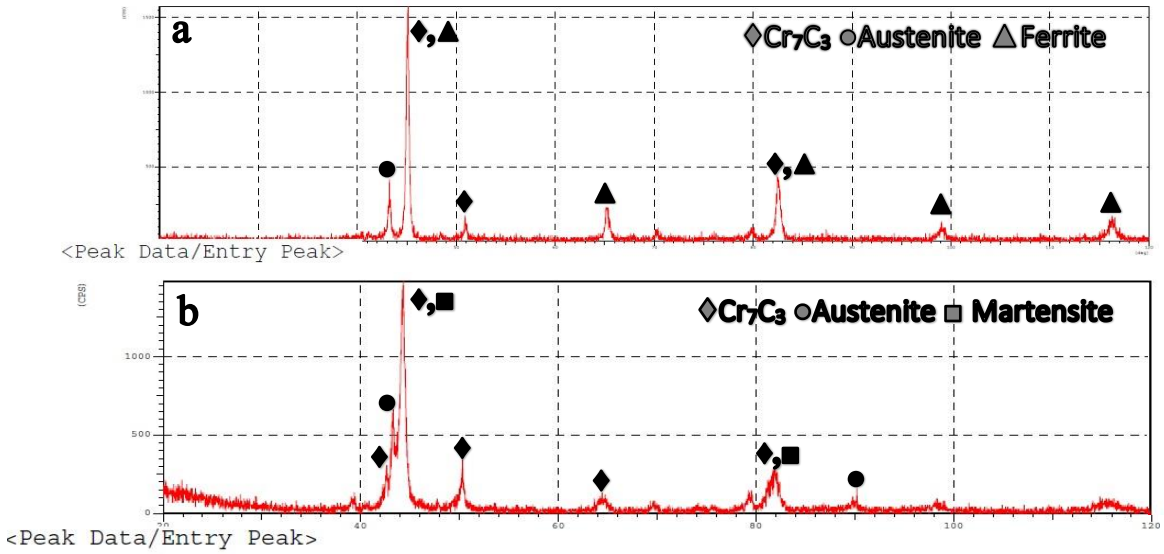

Figure 7 XRD traces indicating phases present in HCWCI microstructure: (a) annealed conditions and (b) after heat treatment at 1100oC and temped at 400oC air cooled (114A).

4. CONCLUSIONS

1) For good erosion resistance for white cast iron 27Cr, the optimal heat treatment process is 3h destabilizing treatment at 1100 ℃, followed by the subsequent 1 h tempering at 400 ℃.

2) Destabilization treatment at 1100°C, as well as at 955°C followed by tempering in 400°C has higher erosive wear resistance than the destabilization treatment at 1100oC and 955°C flowed by tempering in 700°C.

3) In erosive wear, the hardness after work hardening slightly increased from the initial hardness for specimens destabilized at 955°C and 1100°C flowed by tempering heat treatment at 400oC, while specimens destabilized at 955°C and 1100°C flowed by tempering heat treatment at 700°C hardness almost is not increased after erosion test.

4) The main phases after annealing of high Cr white cast iron are Cr7C3, retain austenite and ferrite, while after destabilization t at 1100°C and tempering at 400°C the phases are Cr7C3, retain austenite and martensite.

5. REFERENCES

Al-Bukhaiti, M. A., Ahmed, S. M., Badran, F. M. F., & Emara, K. M. (2007). Effect of impingement angle on slurry erosion behaviour and mechanisms of 1017 steel and high chromium white cast iron. Wear, 262(9), 1187-1198.

Adler, T. A., & Doğan, Ö. N. (1999). Erosive wear and impact damage of high-chromium white cast irons. Wear, 225, 174-180.

ASTM G73-10, Standard Test Method for Liquid Impingement Erosion Using Rotating Apparatus, ASTM International, West Conshohocken, PA, 2010.

ASTM G76-13, Standard Test Method for Conducting Erosion Tests by Solid Particle Impingement Using Gas Jets, ASTM International, West Conshohocken, PA, 2013

Çetinkaya, C. (2006). An investigation of the wear behaviours of white cast irons under different compositions. Materials & design, 27(6), 437-445.

Doğan, Ö. N., Hawk, J. A., & Laird, G. (1997). Solidification structure and abrasion resistance of high chromium white irons. Metallurgical and Materials Transactions A, 28(6), 1315-1328.

Gasan, H., & Erturk, F. (2013). Effects of a destabilization heat treatment on the microstructure and abrasive wear behavior of high-chromium white cast iron investigated using different characterization techniques. Metallurgical and Materials Transactions A, 44(11), 4993-5005.

Higuera-Cobos, O. F., Dumitru, F. D., & Mesa-Grajales, D. H. (2016). Improvement of abrasive wear resistance of the high chromium cast iron ASTM A-532 through thermal treatment cycles. Revista Facultad de Ingeniería, 25(41), 93-103.

Liu, H., Wang, J., Yang, H., & Shen, B. (2008). Effects of cryogenic treatment on microstructure and abrasion resistance of CrMnB high-chromium cast iron subjected to sub-critical treatment. Materials Science and Engineering: A, 478(1), 324-328.

Llewellyn, R. J., Yick, S. K., & Dolman, K. F. (2004). Scouring erosion resistance of metallic materials used in slurry pump service. Wear, 256(6), 592-599.

Sapate, S. G., & Rao, A. R. (2004). Effect of carbide volume fraction on erosive wear behaviour of hardfacing cast irons. Wear, 256(7), 774-786.

Tang, X. H., Chung, R., Pang, C. J., Li, D. Y., Hinckley, B., & Dolman, K. (2011). Microstructure of high (45wt.%) chromium cast irons and their resistances to wear and corrosion. Wear, 271(9), 1426-1431.

Yaer, X., Shimizu, K., Matsumoto, H., Kitsudo, T., & Momono, T. (2008). Erosive wear characteristics of spheroidal carbides cast iron. Wear, 264(11), 947-957.

Zhi, X., Xing, J., Gao, Y., Fu, H., Peng, J., & Xiao, B. (2008). Effect of heat treatment on microstructure and mechanical properties of a Ti-bearing hypereutectic high chromium white cast iron. Materials Science and Engineering: A, 487(1), 171-179.